Serbian Tribology Society

SERBIATRIB '25

19th International Conference on Tribology

Faculty of Engineering
University of Kragujevac

Kragujevac, Serbia, 14 – 16 May 2025

Research paper

DOI:10.24874/ST.25.122

BEHAVIOR OF THE EROSIVE WEAR OF A STEEL PIPELINE SECTION API 5L-X52 BY SOLID PARTICLES OF ALUMINUM OXIDE (AL_2O_3)

Javier Alejandro FRIAS-FLORES[1], Manuel VITE-TORRES[1,*], Ezequiel Alberto GALLARDO-HERNANDEZ[1]

[1]Instituto Politécnico Nacional, Mexico City, Mexico

*Corresponding author: drmanuelvite9@hotmail.com

Abstract: *This study aims to find out the mechanical behaviour of a carbon steel pipeline, API 5L-X52, through the phenomenon of solid particle erosion at different angles of incidence when this is impinged by hard solid particles of aluminium oxide and to analyse the wear process at each angle of incidence. This phenomenon still represents a high-cost loss inside several industries such as aeronautical, mining, extractive, and oil and gas; in these last ones, the ducts and pipelines are the principal element in the fluid transportation, thus these suffer mainly from abrasion and erosion, particularly on the elbow sections of pipelines. Initially, the characterization of both study material and erosive particles was carried out by SEM analysis, EDS, and different mechanical tests to obtain their chemical and physical properties as well as the particle size distribution of erodent particles. Several experimental trials were conducted to determine the mechanical behaviour and wear process, all of them were carried inside of an erosive tribometer, designed according to some parameters of the ASTM G-76 standard, with a particle velocity of 24 m/s at room temperature. After each test, the erosion rate and the mass loss was calculated along with a profilometry analysis of the wear process of the surface, obtaining that the wear behaviour of the pipeline section is as a ductile material. In addition. Finally, severe wear was obtained when the hard particles struck at an angle of incidence of 30°, and the minor wear was at 90°.*

Keywords: *Erosive wear, angle of incidence, alumina, API steel 5L-X52, erosion tribotester*

1. INTRODUCTION

The phenomenon of erosion is a kind of wear where material is removed from the surface by the effect of several hard particles striking it at a certain speed. The kinetic energy that these particles contain due to the velocity at which they are travelling is transferred to the surface, deforming, fracturing or removing the surface layer of material [1,2]. Several factors involved in this phenomenon exist, some of which are dependent on the environmental conditions of the tribology system, others related to the materials involved, but the most relevant are the angle of incidence, velocity of impact and morphology of the incident particles [3,4]. Several research has been conducted to understand the fundamentals of the failures due to this phenomenon, different models and theories have been proposed to predict and reduce their negative effects [5], however, solid particle erosion (SPE) is still causing attention to researchers due to the high impact on costs that this has on different industries [6]. One of the most affected industries by erosion is the oil and gas industry [7], reporting losses of millions of dollars related to erosion and wear problems on components in service, since almost every element in contact with a moving fluid containing hard particles presents erosion of some kind.

On SPE, two types of behavior are expected: the first one is brittle fracture, where cracking formation and fractures are the main mechanisms present on the surface, the second one is ductile, where the surface is worn mainly by cutting and ploughing action as the predominant mechanisms. Brittle behavior is commonly present when the erosion rate has its peak with high angles of incidence, usually 90°; otherwise, ductile behavior is obtained when the highest values of erosion rate are reached with small angles of incidence, around 30° to 45° [8,9,10].

API carbon steel pipelines are widely used in the oil and gas industry as transportation systems over long distances due to their mechanical and chemical resistance and the low manufacturing cost [11]. Several studies have been carried out analyzing the interaction of this material with SPE, slurries [12,13], and in some cases under the effect of the erosion-corrosion phenomena [14,15].

In this study, the behavior of a carbon steel pipeline section, API 5L-X52, under SPE conditions is investigated; to this aim, several specimens are tested under different angles of incidence, evaluating the erosion rate and the mass loss of each one. The angles tested range from 15° to 90° to observe the different wear mechanisms

2. EXPERIMENTAL DETAILS

2.1 Erosive tribotester

The tribotester used for the experimental tests was manufactured by the Tribology Group at Instituto Politécnico Nacional, México, based on some parameters of the ASTM G76 standard [16]. Figure 1 shows a schematic diagram of it. A compressor is used to accelerate tangentially hard particles through the tribotester, an analog gauge maintains and calibrates the air pressure along the tests, a goniometer is used to set the specimens at a specific angle of incidence, and a venturi tube is employed to mix the pressurized air with the hard particles. To define the particle velocity used in the test, the double disk method proposed by Ruff and Ives [17], which gives the relation in equation (1), was used and checked with a high-speed camera. The particle velocity was 24 m/s, several measurements were done with different pressures to get these results. Figure 2 shows the relation between the average particle velocity obtained with each pressure tested.

$$V = \frac{l * \omega}{\theta} \quad (1)$$

Where:

V= Particle velocity [m/s]
L= length separation between discs [m]
ω= angular velocity [rad/s]
ϑ= angular displacement [rad]

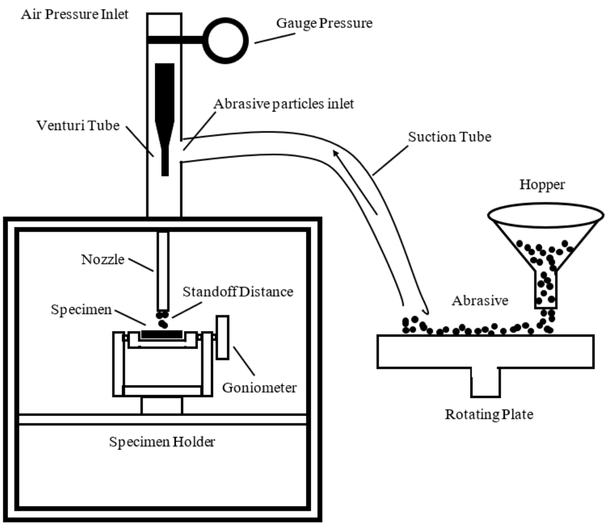

Figure 1. Tribotester schematic diagram

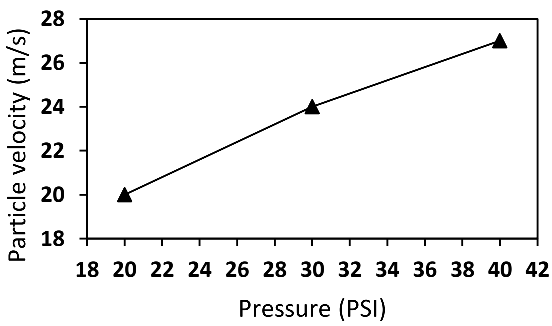

Figure 2. Particle velocities

2.2 Materials

The material tested in this study was a carbon steel API 5L-X52 used in the oil and gas industry to transport materials due to its chemical and physical properties, listed in table 1. This was characterized by Scanning Electron Microscope (SEM) using a JEOL model JSM 7800 microscope and Spectroscopy of X-ray Diffraction; it was obtained its chemical composition as well as images of the microstructure features of the material where can be observed the boundary limits grains and the phases of the material as well, in this case being pearlite and ferrite as expected in a carbon stel, see figure 3. With the X-ray diffraction pattern, it was obtained a crystallography card as carbon steel with the body-centered cubic system (BCC).

Table 1. Physical and chemical properties

Carbon steel API 5L X-52		Alumina	
Physical properties			
Yield strength	420 Mpa	Hardness	2,000 HK
Density	7.72 g/cm^3	Density	3.96 g/cm^3
Hardness	474 HV	Mean particle size	93 µm
Equivalent weight	18.62 gr	Particle shape	Sharpened angular

Chemical properties					
Chemical composition				Chemical composition	
Fe	C	Mn	Si	Al	O
91.83	6.57	1.34	0.25	57.57	42.43

The erodent particles used were alumina (Al_2O_3) due to their chemical and physical properties such as hardness, angular shape and their inert property under some conditions of pressure, temperature, and aggressive chemical conditions. Their characterization was done in the same way that for the tested material, it was used SEM analysis to obtain their chemical composition as well as its morphology and shape, figure 4a; other tests were performed to know its physical properties as nano indentation to know hardness of the particles.

To know the particle size distribution, a laser particle size distribution technique was done using a Beckman Coulter model LS 230 analyzer, the results obtain with this technique are shown in figure 4b. The properties of the erodent particles are listed on table 1 as well.

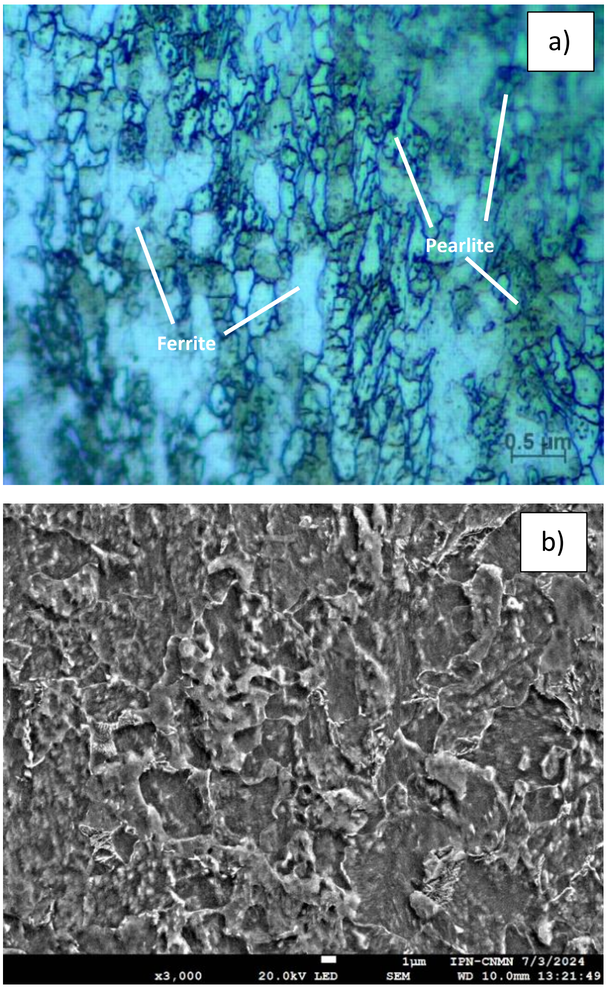

Figure 3. Characteristics of API 5L-X52, a) boundary limits grain, b) SEM image

2.3 Test conditions

All the tests were carried out in room conditions and with a standoff distance between the nozzle, and the specimen of 10±1 mm, the nozzle employed has an outer diameter of 6.1 mm and a length-to-diameter ratio of 20:1 always taken care that the inner diameter of it was not reduced more than 10% as the standard refers. The specimens were machined with a rectangular shape of 30x35 mm and a thickness of 3 mm, polished, cleaned, and weighed before every test. The way the experiments were carried out was in a cumulative loss mass manner, starting with an exposition time of 120s, doubling the test time every time until reaching a total exposure time of 960s with every angle of incidence, testing 15°, 30°, 45°, 60°, and 90°.

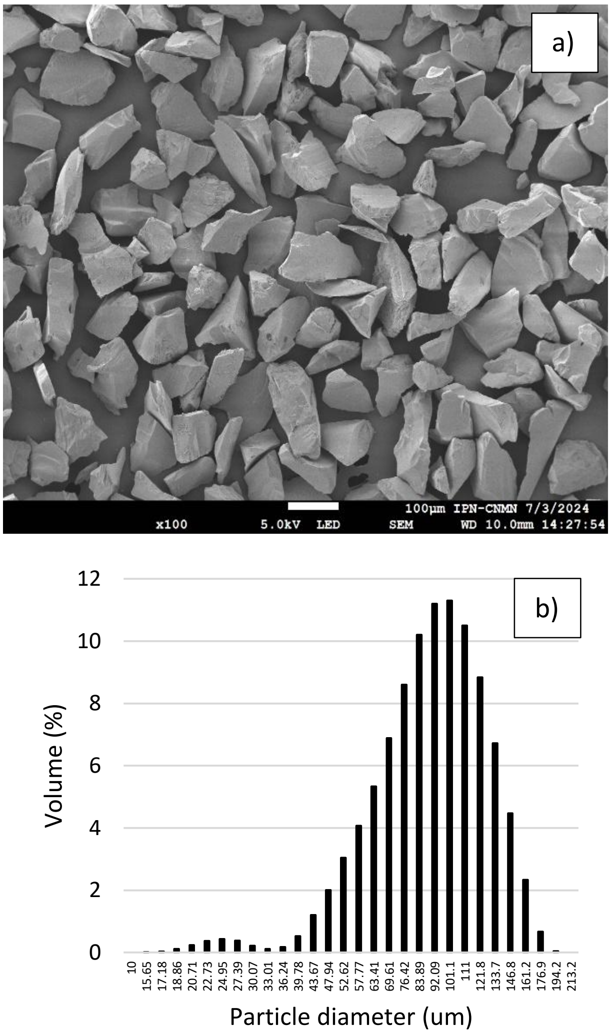

Figure 4. Alumina particles, a) morphology, b) particle size distribution

The mass flow ratio was estimated under the conditions of pressure and particle velocity listed in table 2. To obtain the erosion rate (ER), the equation (2) [18] was implemented, where it is necessary to know the initial and final mass in each test as well as the amount of erosive material used.

$$ER = \frac{\Delta m}{m_a} \qquad (2)$$

Where:

ER= Erosion rate

Δm= Mass difference of every sample after each test [g]

Ma= Abrasive mass used in each test [g]

Table 2. Erosive test conditions

Specimen dimension	30mmx35mm
Thickness	3mm
Roughness (Ra)	0.59 µm
Nozzle diameter	6.1mm
Test temperature	Room temperature
Test time	120s, 240s, 480s and 960s
Angle of incidence	15°, 30°, 45°, 60° and 90°
Average particle velocity	24 m/s
Air pressure	30 PSI
Particles mass flow ratio	101±2 g/min

3. RESULTS AND DISCUSSION

3.1 Mass loss

The effect that the angle of incidence could have on mass loss is shown in figure 5, here can be observed that the lowest value of mass loss is at 90°, with higher angles of incidence, in accordance with the requirements of the material to resist perpendicular impacts of hard particles, otherwise, it was obtained the higher mass loss with angles of incidence of 30° and 45°, indicating that the material is prone to thinning the duct walls when particles impact at low angles of incidence or when the fluid has a more laminar tendency. This indicates the material tends to exhibit a ductile behavior more than fragile [9].

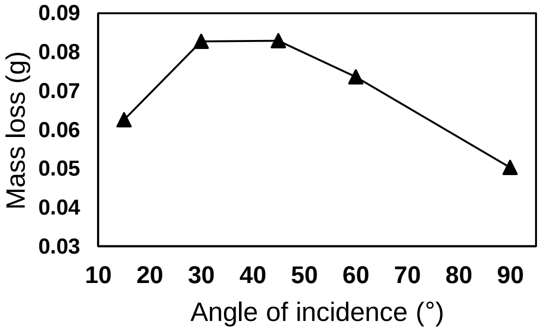

Figure 5. Mass loss as a function of the angle of incidence

3.2 Erosion rate

The effect of the angle of incidence on the erosion rate can be observed in figure 6, where the ER drops as the angle of incidence increases having their maximum values at 30° and 45°, this condition indicate that the material has a ductile behavior according the literature [19,20], also its mentioned that a ductile material suffer cutting on surface as results of the erodent particles sliding on the surface having high rates of plastic deformation regardless the shape of the erodent [21,22]. On factor to these results is that with low angles of incidence the rebounding effect is lower than at higher angles, so, more particles strike the surface at low angles having a higher mass loss and an ER, meanwhile at 90° the particles rebounding and impact each other causing fewer mass loss and lower ER. Figure 7 exhibits the ER behavior along the test, where it tends to stabilize with time, only having a peak at the beginning of the test, irrespective of the angle of incidence.

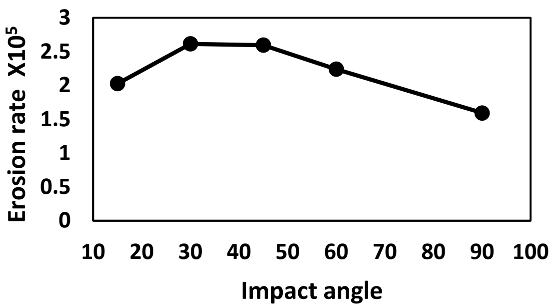

Figure 6. Erosion rate depending on the angle of incidence

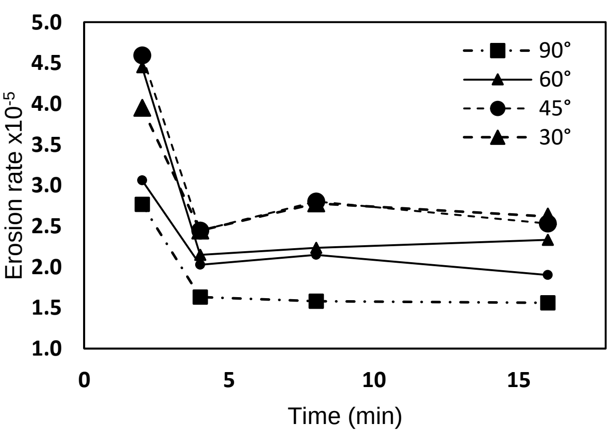

Figure 7. Erosion rate vs time

3.3 Profilometry

A profilometry study, using a Mitutoyo profilometer model CV-500, was conducted to observe the wear progression and the depth and distance of the wear scars depending on the angle of incidence, as shown in figure 8. It was obtained that the higher the angle, the shorter the distance of the scar, having a wear scar length of 12 mm at 90°, increasing gradually until reaching a scar length greater than 25 mm at 15°. Although the deepest valley was obtained at 60° with a depth of 0.164mm, the maximum ER was obtained at 30° and 45° with a depth of 0.145 mm and 0.138 mm, respectively. This is another factor that contributes to the ER; the depth and length of the scars affect mass loss and in consequently, the ER. The area of impact at 30° and 45°, the highest ER, has an oval shape which represents a bigger area to strike, whereas, at 90° was the smallest ER having a circular shape with smaller diameter, this can be seen on figure 9 along with the evolution of the wear scar.

3.4 Erosive mechanisms

In erosion phenomenon different wear mechanisms act synergically and interact one with another, which complicates identify each mechanism by itself but in a general way some mechanisms predominate at high angles of incidence rather than others that are more present at low angles. With high angles, almost all kinetic energy in the particles is used to penetrate, deform and fracture the material surface, therefore, the most common process to lose material with these angles is protrusions or fracture due to the impact of particles which results in lips of ridges (displace material) and the subsequent fracture of these lips by the impact of more particles. Also, cutting effects are observed in this situation, as can be seen in the figure. 10a, where some of these mechanisms are pointed out.

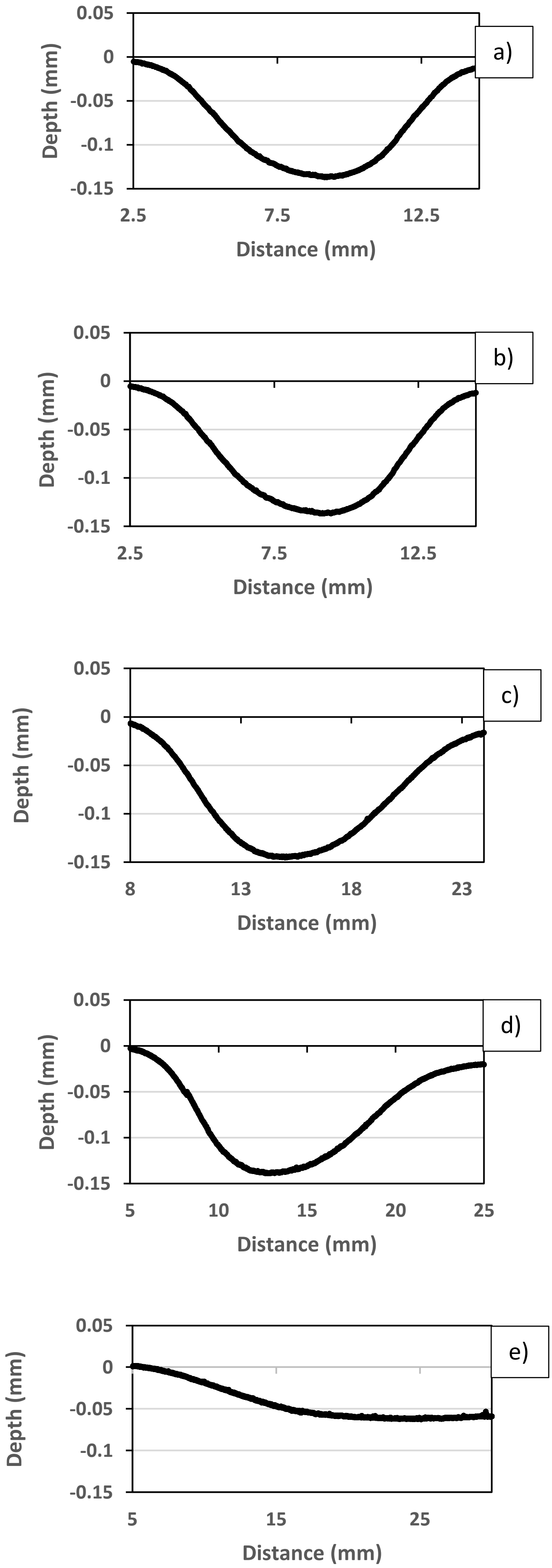

Figure 8. Scar wear profilometry after 960s, a) 90°, b) 60°, c) 45°, d) 30° and e) 15°

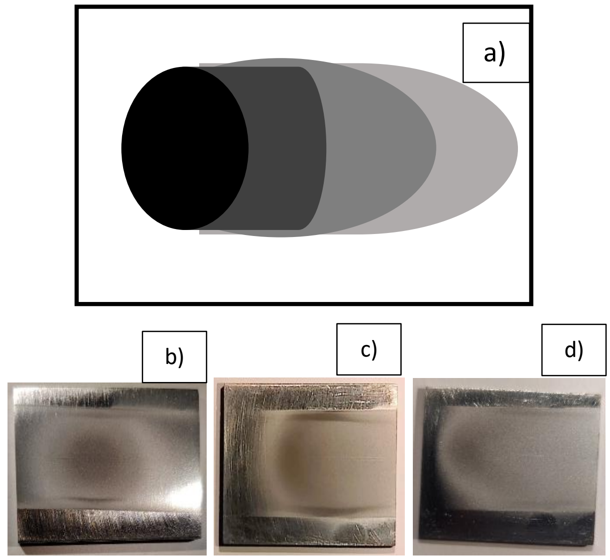

Figure 9. Erosion scars, a) evolution diagram, b) erosion scar at 90°, c) erosion scar at 45° and d) erosion scar at 15°

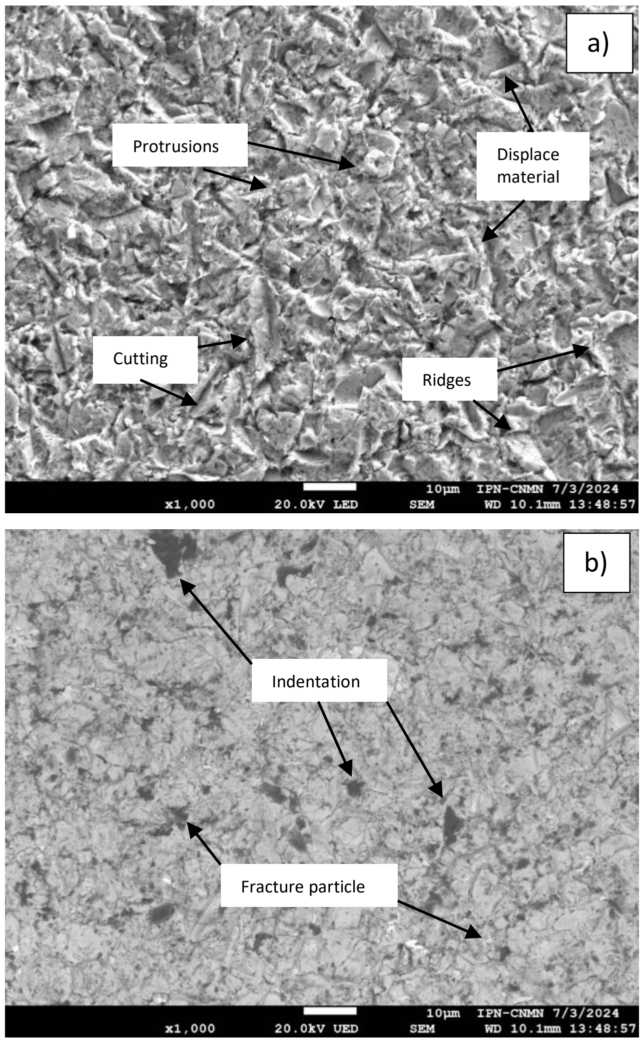

Figure 10. Samples strike at 90, SEM images at x1000, a) worn surface material, b) particles embebbed in the material.

Another contribution to the ER on this topic is that the embedded particles resulting from impacts at high angles of incidence form a protective layer to other particles, limiting the erosion capacity of the erodent and adding extra weight to the sample, these embedded particles can be observed in Fig. 11b.

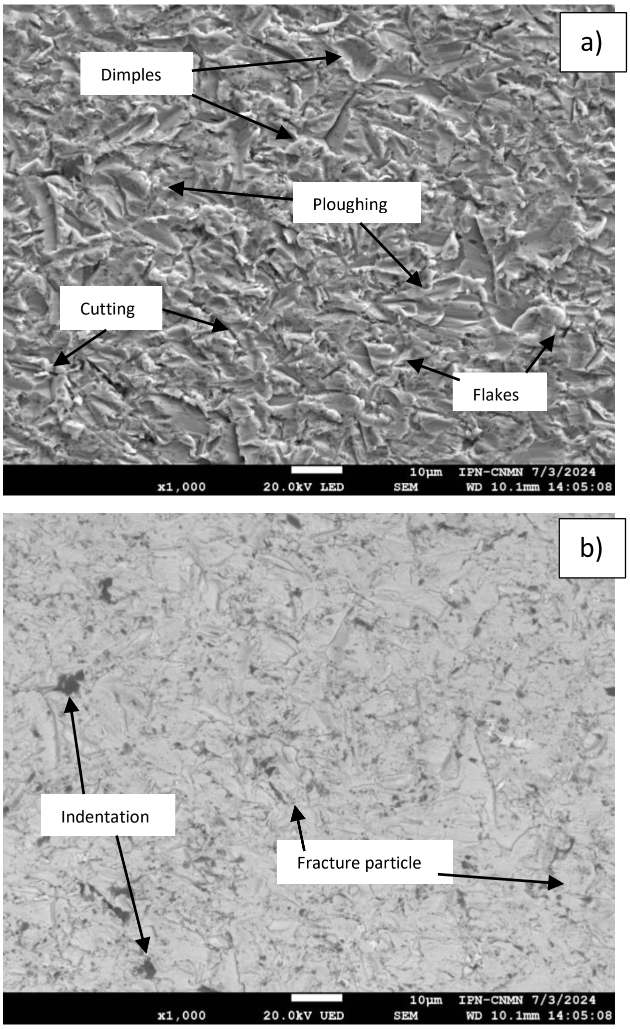

Figure 11. SEM images at x1000 samples strikes at 15°, a) wear mechanisms, b) embedded particles

When hard particles strike samples at low angles of incidence, the remotion mechanism is different; the dominant mechanism is ploughing [23], Where the kinetic energy of the particles divides into its components, the y-axis component penetrates the surface while the x-axis component slides on the surface. As the particles slide and hit the surface displace material ahead and to the sides forming dimples and the so-called flakes, which with the posterior impact or more particles, are flattened or fractured, leading to remotion of material as the later stage of the erosion process, some of these mechanisms can be observed in figure. 11a, where the sample struck at 15° is shown. In figure 11b, some embedded particles can be seen, fewer than those observed at 90°, confirming the little addition of material to the samples when low angles of incidence are used.

4. CONCLUSIONS

1. Erosion rate depends on the behavior of the material, ductile or brittle, in this case, a ductile behavior, which indicates that the maximum erosion rates are reached with low angles of incidence. in this study, the maximum erosion rates were reached at 30°.
2. This material has better performance when it is attacked under a normal angle to the surface, due to its ductile behavior; therefore, elbow sections are more prone to resist normal impact on sections when particles strike with an angle around 90°.
3. It was found that the initial erosion rate, at 120s, regardless of the angle of incidence, exhibits higher values than tests with a higher exposure time. All tests have an initial erosion rate, and with the subsequent tests, this value tends to stabilize with time. This could be explained cause the repetitive impact of hard particles causes a plastic deformation on the material, which leads to a hardening of the surface, increasing wear resistance. Additionally, some particles are embedded, forming a protective layer against the next impacts. In this study, the maximum initial erosion rate was obtained at 60° and 40°.
4. It was determined that the main wear mechanism to generate material removal is ploughing, flake formation, ridges, and plastic deformation. These mechanisms, together with repetitive impacts, cause higher mass loss at low angles of incidence.

ACKNOWLEDGEMENT

The authors thank the Department of Research and Graduate Studies (SIP) of the National Polytechnic Institute, Mexico.
To the honorable memory of Dr. Jaime Vite-Torres, member of the Tribology Group of the ESIME of Zacatenco, IPN.

ORCID iDs

Javier Alejandro FRIAS-FLORES 0009-0008-0002-6717
Manuel VITE-TORRES 0000-0003-1502-0189
Ezequiel Alberto GALLARDO-HERNANDEZ 0000-0001-5004-7999

REFERENCES

[1] I. Hutchings and R. Winter, "Particle erosion of ductile metals: A mechanism of material removal," Wear, vol. 27, no. 1, pp. 121–128, 1974, doi: 10.1016/0043-1648(74)90091-x.
[2] A. Alhussein, J. Capelle, J. Gilgert, S. Dominiak, and Z. Azari, "Influence of sandblasting and hydrogen on tensile and fatigue properties of pipeline API 5L X52 steel," International Journal of Hydrogen Energy, vol. 36, no. 3, pp. 2291–2301, 2010, doi: 10.1016/j.ijhydene.2010.11.081.
[3] M. Liebhard and A. Levy, "The effect of erodent particle characteristics on the erosion of metals," Wear, vol. 151, no. 2, pp. 381–390, 1991, doi: 10.1016/0043-1648(91)90263-t.
[4] M. A. Islam and Z. N. Farhat, "Effect of impact angle and velocity on erosion of API X42 pipeline steel under high abrasive feed rate," Wear, vol. 311, no. 1–2, pp. 180–190, 2014, doi: 10.1016/j.wear.2014.01.005.
[5] D. O'Flynn, M. Bingley, M. Bradley, and A. Burnett, "A model to predict the solid particle erosion rate of metals and its assessment using heat-treated steels," Wear, vol. 248, no. 1–2, pp. 162–177, 2001, doi: 10.1016/s0043-1648(00)00554-8.
[6] M. Vite-Torres et al., "Study of solid particle erosion on AISI 420 stainless steel using angular silicon carbide and steel round grit particles," Wear, vol. 301, no. 1–2, pp. 383–389, 2013, doi: 10.1016/j.wear.2013.01.071.
[7] H. Arabnejad, A. Mansouri, S. Shirazi, and B. McLaury, "Abrasion erosion modeling in particulate flow," Wear, vol. 376–377, pp. 1194–1199, 2017, doi: 10.1016/j.wear.2017.01.042.
[8] I. Finnie, "Erosion of surfaces by solid particles," Wear, vol. 3, no. 2, pp. 87–103, 1960, doi: 10.1016/0043-1648(60)90055-7.
[9] D. Aquaro and E. Fontani, "Erosion of ductile and brittle material," Meccanica, vol. 36, no. 6, pp. 651–661, 2001, doi: 10.1023/a:1016396719711.
[10] E. E. Vera-Cárdenas et al., "Solid particle erosive wear study of polymer composite materials for wind turbine applications," Polymer Composites, vol. 42, no. 4, pp. 1988–1999, 2021, doi: 10.1002/pc.25950.
[11] Y. Xu, Q. Zhang, H. Chen, and Y. Huang, "Understanding the interaction between erosion and corrosion of pipeline steel in acid solution of different pH," Journal of Materials Research and Technology, vol. 25, pp. 6550–6566, 2023, doi: 10.1016/j.jmrt.2023.07.109.
[12] R. Mohsin, Z. Majid, and M. Yusof, "Multiple failures of API 5L X42 natural gas pipe: Experimental and computational analysis," Engineering Failure Analysis, vol. 34, pp. 10–23, 2013, doi: 10.1016/j.engfailanal.2013.07.007.
[13] Z. Majid, R. Mohsin, Z. Yaacob, and Z. Hassan, "Failure analysis of natural gas pipes," Engineering Failure Analysis, vol. 17, no. 4, pp. 818–837, 2009, doi: 10.1016/j.engfailanal.2009.10.016.
[14] X. Hu and A. Neville, "CO_2 erosion–corrosion of pipeline steel (API X65) in oil and gas conditions—A systematic approach," Wear, vol. 267, no. 11, pp. 2027–2032, 2009, doi: 10.1016/j.wear.2009.07.023.
[15] D. Ramírez-Arreola et al., "Influence of swirl number and incidence angle on erosion-corrosion behavior of API 5L X-52 steel under swirling jets," Wear, vol. 510–511, p. 204518, 2022, doi: 10.1016/j.wear.2022.204518.
[16] ASTM G76-18, Standard Test Method for Conducting Erosion Test by Solid Particle Impingement Using Gas Jets, ASTM International.
[17] A. Ruff and L. Ives, "Measurement of solid particle velocity in erosive wear," Wear, vol. 35, no. 1, pp. 195–199, 1975, doi: 10.1016/0043-1648(75)90154-4.
[18] C. S. La Rosa et al., "Effect of tangential velocity on erosion of ASTM A-106 Grade B steel pipe under turbulent swirling impinging jet," Tribology International, vol. 113, pp. 500–506, 2017, doi: 10.1016/j.triboint.2017.01.011.
[19] I. Finnie, G. Stevick, and J. Ridgely, "The influence of impingement angle on the erosion of ductile metals by angular abrasive particles," Wear, vol. 152, no. 1, pp. 91–98, 1992, doi: 10.1016/0043-1648(92)90206-n.
[20] Y. Oka, H. Ohnogi, T. Hosokawa, and M. Matsumura, "The impact angle dependence of erosion damage caused by solid particle

impact," Wear, vol. 203–204, pp. 573–579, 1997, doi: 10.1016/s0043-1648(96)07430-3.
[21] J. Bitter, "A study of erosion phenomena. Part I," Wear, vol. 6, no. 1, pp. 5–21, 1963, doi: 10.1016/0043-1648(63)90003-6.
[22] J. Bitter, "A study of erosion phenomena. Part II," Wear, vol. 6, no. 3, pp. 169–190, 1963, doi: 10.1016/0043-1648(63)90073-5.
[23] I. Hutchings, "A model for the erosion of metals by spherical particles at normal incidence," Wear, vol. 70, no. 3, pp. 269–281, 1981, doi: 10.1016/0043-1648(81)90347-1.